NudE and NudEL are required for mitotic progression and are involved in dynein recruitment to kinetochores

Stephanie A. Stehman, Yu Chen, Richard J. McKenney, and Richard B. Vallee

Department of Pathology and Cell Biology, Columbia University, New York, NY 10032

NudE and NudEL are related proteins that interact with cytoplasmic dynein and LIS1. Their functional relationship and involvement in LIS1 and dynein regulation are not completely understood. We find that NudE and NudEL each localize to mitotic kinetochores before dynein, dynactin, ZW10, and LIS1 and exhibit additional temporal and spatial differences in distribution from the motor protein. Inhibition of NudE and NudEL caused metaphase arrest with misoriented chromosomes and defective microtubule attachment. Dynein and dynactin were both displaced from kinetochores by the injection of an anti-NudE/NudEL antibody. Dynein but not dynactin interacted with NudE surprisingly through the dynein intermediate and light chains but not the motor domain. Together, these results identify a common function for NudE and NudEL in mitotic progression and identify an alternative mechanism for dynein recruitment to and regulation at kinetochores.

Introduction

Cytoplasmic dynein is a multisubunit complex that functions as a minus end–directed microtubule motor and plays critical roles in a variety of eukaryotic cellular functions, including retrograde axonal transport (Paschal and Vallee, 1987) and directed cell migration (Dujardin et al., 2003). In addition, cytoplasmic dynein is involved in numerous aspects of mitosis, such as spindle pole organization, spindle orientation (Busson et al., 1998; Faulkner et al., 2000; O'Connell and Wang, 2000), and mitotic checkpoint regulation (Smith et al., 2000; Howell et al., 2001; Wojcik et al., 2001).

Dynein behavior is mediated by numerous factors, including the dynactin complex, as well as by an additional group of regulatory proteins initially identified in *Aspergillus nidulans*. The *NudF* gene in *A. nidulans* was found to be homologous to human LIS1, which causes the brain developmental disease type I lissencephaly when mutated (Xiang et al., 1995). This condition results from defects at several stages in the pathway of neurogenesis and migration in the neocortex and involves defects in both cell division and migration (Tsai et al., 2005). In vitro studies of LIS1 have revealed that it interacts physically with both cytoplasmic dynein and dynactin. Furthermore, LIS1 colocalizes with dynein at multiple subcellular sites, including the centro-

some, kinetochores, mitotic cortex, and the leading edge of migrating cells (Faulkner et al., 2000; Dujardin et al., 2003).

In addition to LIS1, *NudE* and *NudC* were also identified in the *A. nidulans* dynein pathway. *NudE* was first identified as a multicopy suppressor of *NudF* (Efimov and Morris, 2000) and has two mammalian homologues, NudE and NudEL (gene names *Nde1* and *Ndel1*, respectively), which were identified in LIS1 two-hybrid screens (Feng et al., 2000; Sasaki et al., 2000). These proteins are 55% identical in full-length sequence and are similar in both size and predicted secondary structure. Each interacts with LIS1 through a predicted N-terminal coiled-coil region (Efimov and Morris, 2000; Feng et al., 2000; Niethammer et al., 2000) and with cytoplasmic dynein through a globular C-terminal domain (Niethammer et al., 2000; Sasaki et al., 2000; Liang et al., 2004). NudEL was reported to interact with the dynein motor domain by yeast two-hybrid and coexpression assays, suggesting a potential role in dynein motor regulation (Sasaki et al., 2000).

In spite of the structural similarities between NudE and NudEL, recent studies have revealed surprisingly different phenotypes in knockout mice. Homozygous *NudE*-null mice are viable but display a microcephalic, or small brain, phenotype predominantly affecting the cerebral cortex (Feng and Walsh, 2004). An increase in mitotic index as well as spindle defects was reported in the developing brain, implying that NudE, like LIS1 (Faulkner et al., 2000), participates in cell division. In contrast, *NudEL*-null

Correspondence to Richard B. Vallee: rv2025@columbia.edu

Abbreviation used in this paper: CENP, centrosome protein.

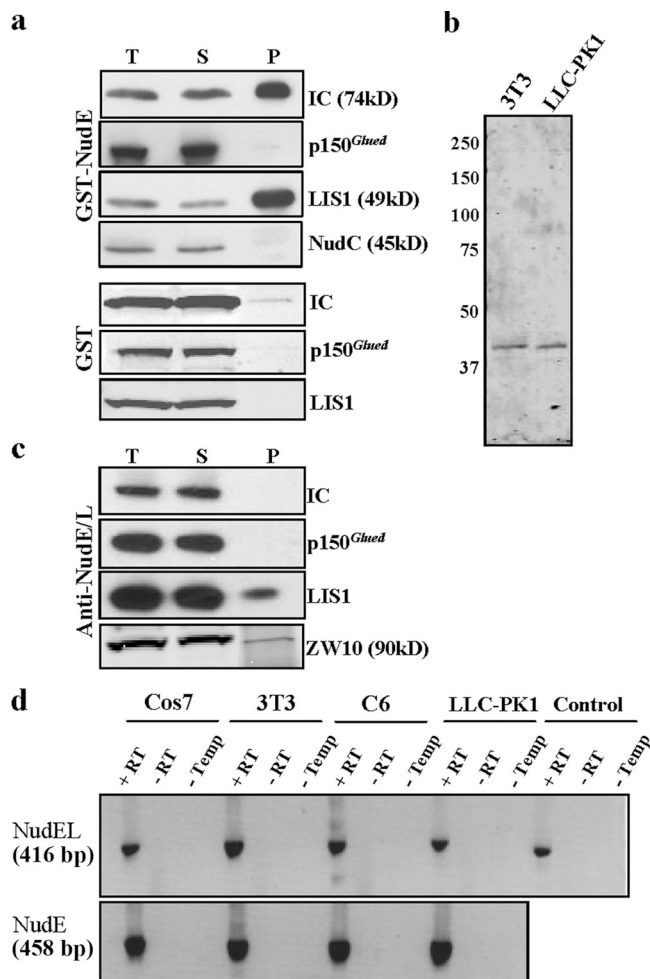The online version of this article contains supplemental material.

Figure 1. **Biochemical analysis of NudE and NudEL.** (a) Recombinant GST-NudE was used to pull down interacting proteins from bovine brain extract, which were visualized by immunoblotting. The GST-NudE–bound cytoplasmic dynein intermediate chain (IC) and LIS1. No interaction was seen with dynactin (p150^{Glued}) or NudC. T, total; S, supernatant; P, pellet. (b) Immunoblotting of 3T3 and LLC-PK1 cell lysates using the NudE/NudEL polyclonal antibody produced in this study reveals one major immunoreactive band at 43 kD. (c) Immunoprecipitation from bovine brain extract using the anti-NudE/NudEL antibody coprecipitates LIS1 and ZW10 but not dynein or dynactin. (d) RT-PCR was used to determine the presence of NudE and NudEL in the cell lines used by this study. All lines were positive for both NudE and NudEL in the presence of reverse transcriptase (+RT). Bands represent an amplicon of 416 bp for NudEL and 458 bp for NudE. No bands were evident in control samples lacking reverse transcriptase (−RT) or template (−temp). Detection of the constitutively expressed *rig/S15* gene was used as a positive control.

mice exhibited early embryonic lethality (Sasaki et al., 2005), a phenotype similar to that of both LIS1 (Hirotsune et al., 1998) and cytoplasmic dynein (Harada et al., 1998). However, hypomorphic mutants exhibited defects not in cell division but in neuronal distribution (Sasaki et al., 2005), supporting previous RNAi data to this effect (Shu et al., 2004).

Both proteins have been localized to the centrosome (Feng et al., 2000; Sasaki et al., 2000). Yeast two-hybrid data have identified interactions between NudE and several centrosomal proteins (Feng et al., 2000), whereas coimmunoprecipitation studies identified γ-tubulin as an additional binding partner (Feng et al., 2000; Liang et al., 2004). NudEL has also been

implicated in dynein-mediated vesicular transport (Liang et al., 2004), although localization of NudEL to membranous organelles has not been demonstrated. Additionally, NudE has been reported to localize to punctate structures within the mitotic spindle that were thought to be kinetochores (Feng and Walsh, 2004), although the extent to which the distribution of NudE overlapped with that of LIS1 and dynein was not examined.

We initiated this study to determine the extent to which NudE and NudEL function in concert with LIS1, dynein, and dynactin and to test the degree to which NudE and NudEL differ functionally from each other. We find that both NudE and NudEL associate with mitotic kinetochores but arrive at these sites well in advance of dynein, LIS1, dynactin, and ZW10. The inhibition of NudE and NudEL function prevents dynein, dynactin, and LIS1 localization to kinetochores, leading to metaphase arrest and kinetochore misorientation. Finally, we find that NudE interacts with the dynein complex surprisingly through its tail, or stem, domain and shows no interaction with dynactin. These results identify a novel mechanism for kinetochore dynein recruitment and suggest important roles for NudE and NudEL in kinetochore assembly and microtubule attachment.

Results

Biochemical analysis of NudE and NudEL

NudE and NudEL have been reported to interact with cytoplasmic dynein and LIS1 (Efimov and Morris, 2000; Niethammer et al., 2000; Sasaki et al., 2000; Smith et al., 2000; Liang et al., 2004). We find that bacterially expressed GST-tagged full-length NudE pulls down LIS1 and dynein from bovine brain extract (Fig. 1 a). However, in contrast to LIS1 (Faulkner et al., 2000; Smith et al., 2000), we observe no detectable interaction with dynactin or NudC (Fig. 1 a). Additionally, we found the dynein/dynactin-interacting protein ZW10 bound to NudE, biochemically (Fig. 1 c) confirming an interaction previously identified in a ZW10 yeast two-hybrid screen (Starr et al., 2000).

To examine the distribution and in vivo functional properties of NudE, we produced a polyclonal antibody against the full-length protein mNudE. We find that the antibody recognizes a 43-kD band in 3T3, C6, LLC-PK1, MDCK, and COS7 cell lysates (Fig. 1 b and not depicted). Interestingly, recombinant NudE and NudEL each reacted with the antibody (Fig. S1, available at http://www.jcb.org/cgi/content/full/jcb.200610112/DC1), which is consistent with their extended sequence homology. In addition to the major NudE/NudEL band at 43 kD, we occasionally detected additional bands at 75 and 105 kD, as has been previously reported for an anti-NudE antibody (Feng et al., 2000); however, they are eliminated along with the major NudE/NudEL band by preadsorption against GST-NudE (Fig. S1), suggesting that they represent SDS-insensitive NudE and NudEL aggregates (Feng et al., 2000). To determine the reactivity of the antibody under native conditions, we tested its behavior by immunoprecipitation. Despite the ability of recombinant NudE to pull down dynein, LIS1, and ZW10 (Fig. 1 a), the antibody coimmunoprecipitated only the latter two proteins (Fig. 1 c). This observation suggests that the antibody selectively blocks only the interaction of NudE and NudEL with dynein.
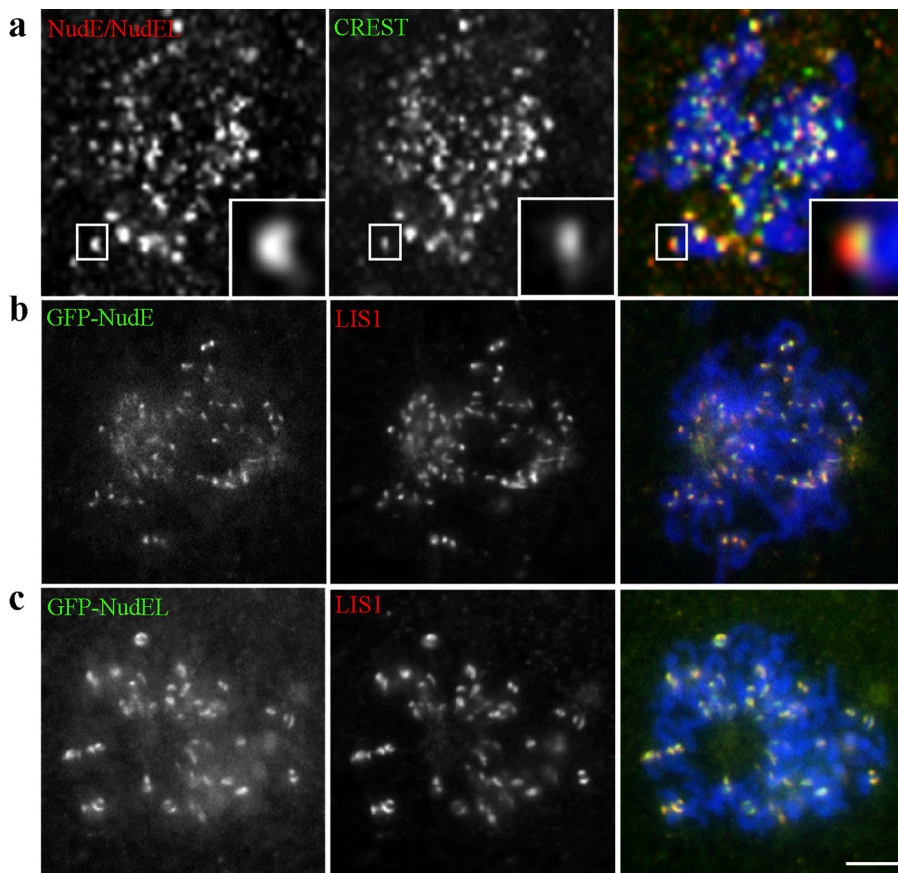
Figure 2. **NudE and NudEL localize to mitotic kinetochores.** (a) Immunofluorescence microscopy using our anti-NudE/NudEL antibody reveals reactivity with mitotic kinetochores in COS7 epithelial cells, as identified by costaining with CREST autoimmune serum. NudE/NudEL localization can be observed at the outer region of the kinetochore relative to CREST (insets), which is known to stain the inner kinetochore region. (b and c) GFP-NudE (b) and GFP-NudEL (c) were expressed in COS7 epithelial cells. The cells were treated with nocodazole to depolymerize microtubules and were examined by immunofluorescence microscopy. Each of the fusion proteins colocalized with LIS1 at kinetochores. Bar, 5 μM.

The differential expression of NudE and NudEL during brain development has been reported (Feng et al., 2000; Sasaki et al., 2000), but the extent to which expression overlaps in individual cell types has not been explored. To examine this issue, we conducted RT-PCR in 3T3, C6, LLC-PK1, and COS7 cell lysates. As seen in Fig. 1 d, both proteins were expressed in all cell lines examined.

Subcellular localization of NudE and NudEL

NudE and NudEL have been found to localize to centrosomes in interphase cells (Feng et al., 2000; Niethammer et al., 2000; Sasaki et al., 2000; Yan et al., 2003) and to participate in vesicular transport (Liang et al., 2004). Additionally, NudE was reported to localize to punctate structures within the mitotic spindle, which may be kinetochores (Feng and Walsh, 2004). To define the distribution of these proteins more fully and to test the extent to which they function in concert with cytoplasmic dynein, dynactin, and LIS1, we examined their distribution throughout the cell cycle, with particular emphasis on mitosis.

Immunofluorescence staining using our NudE/NudEL antibody in COS7 cells showed colocalization with CREST human autoimmune serum on mitotic kinetochores (Fig. 2 a). To test whether this localization pattern reflected the behavior of NudE, NudEL, or both, each protein was expressed as a GFP fusion. GFP-NudE and GFP-NudEL each colocalized with LIS1 at mitotic kinetochores, a pattern observed in nocodazole-treated (Fig. 2, b and c) and untreated (not depicted) COS7 epithelial cells. At high magnification, the NudE and NudEL staining pattern

was slightly shifted from that of the CREST autoimmune signal, indicating that NudE and NudEL localize to the outer region of the kinetochore (Fig. 2 a, insets). Additionally, when cells were treated with nocodazole before fixation, NudE and NudEL (Fig. 2, b and c) accumulated in a crescent pattern, which is a characteristic common to outer kinetochore proteins, including dynein and LIS1 (Echeverri et al., 1996; Faulkner et al., 2000; Hoffman et al., 2001).

Despite these localization similarities, we identified striking differences in the timing with which NudE and NudEL appeared and departed from mitotic kinetochores in comparison with dynein, dynactin, and LIS1. Immunofluorescence microscopy revealed strong NudE/NudEL kinetochore staining during prophase before either dynein, dynactin, or LIS1 (Figs. 3 a and S2 a, available at http://www.jcb.org/cgi/content/full/jcb .200610112/DC1), suggesting that NudE/NudEL localization to mitotic kinetochores occurs independently of dynein. Furthermore, NudE and NudEL each remained at the kinetochore until early anaphase, well after dynein and LIS1 had departed (Figs. 3 a and S2 a). Surprisingly, GFP-NudE (unpublished data) and -NudEL (Figs. 3 c and S2 b) also preceded ZW10 at kinetochores, although each of these proteins departed at a similar stage of mitosis.

Cells were examined for cortical NudE and NudEL staining, as has previously been observed during mitosis for cytoplasmic dynein (Busson et al., 1998) and LIS1 (Faulkner et al., 2000). We found NudE and NudEL to be absent from the mitotic cortex (Fig. 3 d). In contrast, NudE/NudEL showed strong localization
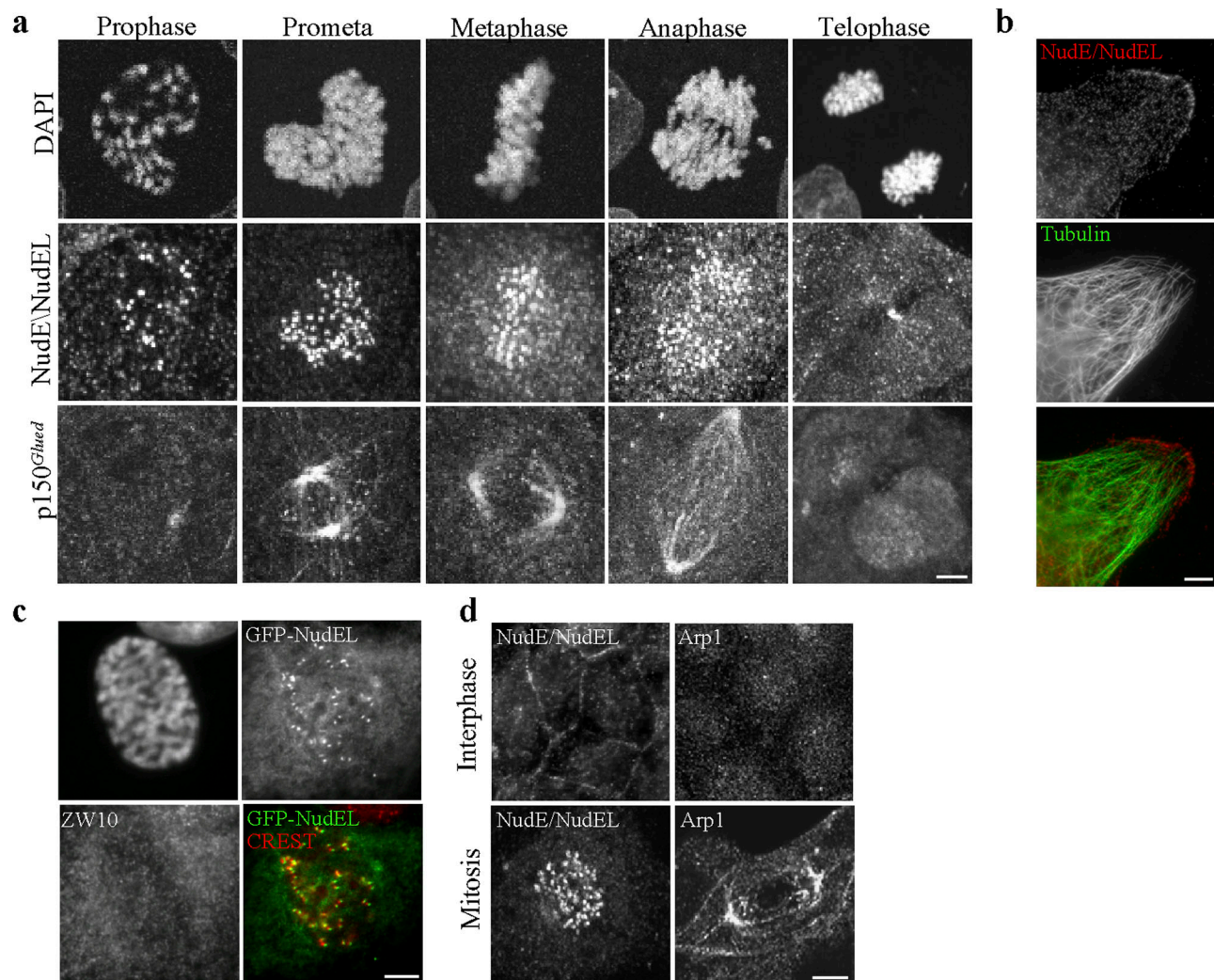
Figure 3. **NudE/NudEL show distinct subcellular patterns of localization in comparison with dynein, dynactin, and LIS1.** (a) Immunofluorescence analysis of NudE/NudEL in MDCK cells was used to examine the distribution of the endogenous proteins throughout mitosis. NudE/NudEL immunoreactivity was clearly present at kinetochores by prophase and persisted until early anaphase. Dynactin (p150^{glued}) staining appeared at prometaphase and was lost by metaphase. (b) Immunofluorescence analysis of NudE/NudEL reveals staining at the leading edge of migrating NIH3T3 fibroblasts after wounding. (c) In an LLC-PK1 cell line stably expressing GFP-NudEL, localization of the fusion protein at mitotic kinetochores was readily detected at prophase colocalizing with CREST before ZW10. (d) Immunofluorescence analysis of NudE/NudEL in MDCK cells reveals distinct patterns of cortical localization in comparison with dynactin (Arp1). During interphase, NudE/NudEL localize prominently to the cortex in regions of cell–cell contact, whereas Arp1 staining is not observed at these sites. Conversely, Arp1 was found associated with the metaphase/anaphase cell cortex, where NudE/NudEL were not detected. Bars, 5 μM.

to the cortex of partially polarized interphase MDCK epithelial cells, where we did not detect dynein or dynactin (Fig. 3 d). We also observed strong staining at the leading edge of migrating NIH3T3 fibroblasts in wounded monolayers (Fig. 3 b), as we have previously observed for LIS1, dynein, and dynactin (Dujardin et al., 2003). We found no evidence of NudE/NudEL accumulation at microtubule plus ends as has been seen in other systems (Li et al., 2005; Efimov et al., 2006).

Phenotypic analysis of NudE

These data revealed similarities but also interesting differences in the distribution of NudE and NudEL from that of dynein, dynactin, and LIS1. Furthermore, we found that the localization patterns for NudE and NudEL were indistinguishable at mitotic kinetochores, suggesting that these proteins may have common cellular functions. NudE and NudEL RNAi has been shown to

result in cell death (Liang et al., 2004; Hirohashi et al., 2006; our unpublished data). As an alternative approach, we examined the behavior of cells expressing NudE fragment (Fig. 4 a). Overexpression of an N-terminal fragment of NudE has been reported to interfere with mitosis (Feng and Walsh, 2004). As in a previous study (Feng and Walsh, 2004), we observe severe defects in mitotic spindle organization after the overexpression of an N-terminal NudE fragment (GFP-NudE-C188) but found no effect on spindle organization with a C-terminal fragment (GFP-NudE-N189) containing the dynein-binding region or with empty vector controls (Fig. 4 c). To gain further insight into the effects of these fragments on mitotic behavior, we monitored transfected cells by live imaging. Not unexpectedly in view of the fixed cell analysis, the N-terminal fragment caused a variety of effects, including multipolar divisions and prometaphase arrest (unpublished data). Surprisingly, overexpression of the C-terminal fragment had a
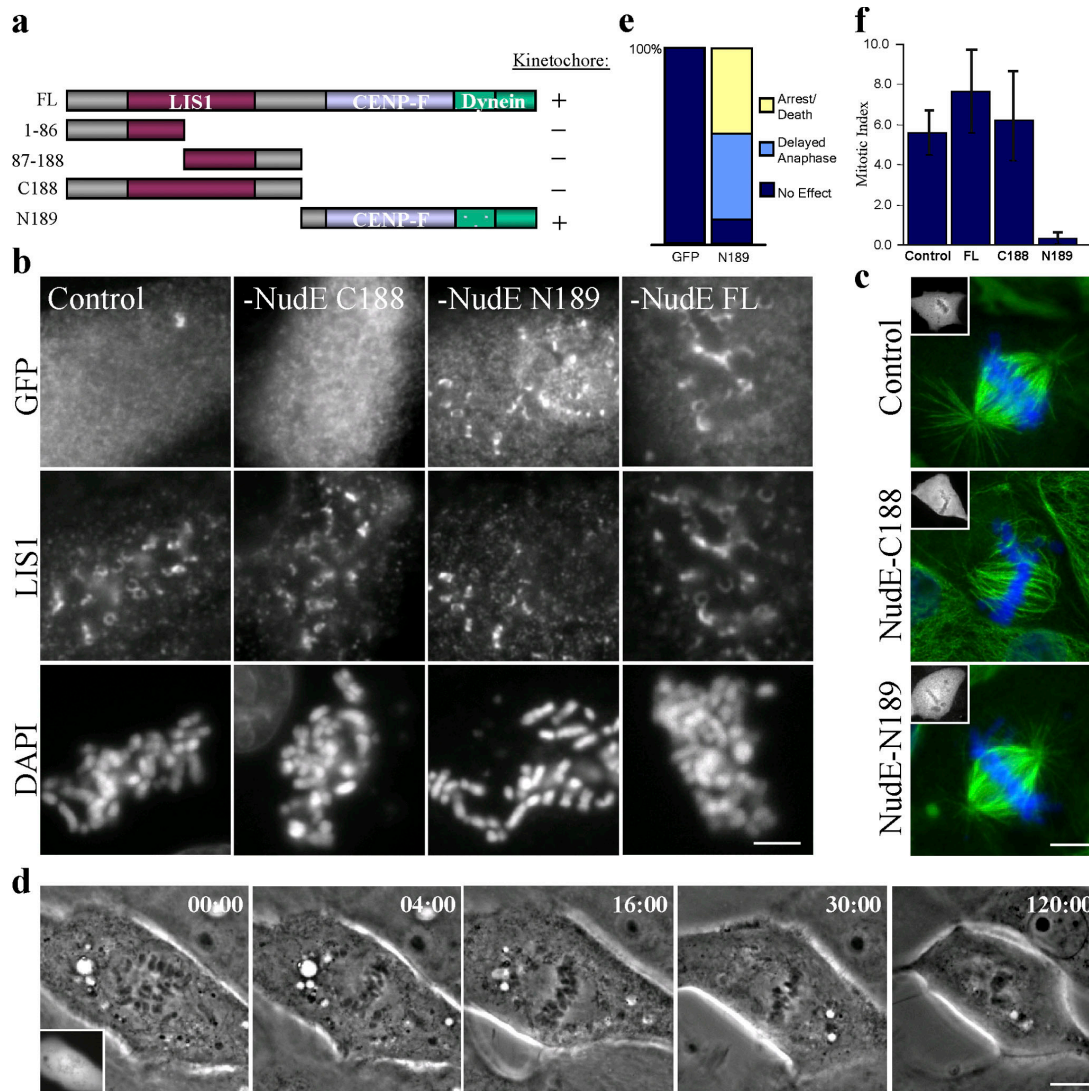
Figure 4. **Behavior and mitotic effects of NudE fragments.** (a) Diagram of NudE-binding domains and deletion fragments used in this study: LIS1-binding domain (aa 56–166), CENP-F–binding domain (aa 192–323), and dynein-binding domain (aa 256–344). (b) Kinetochore association of full-length and truncated NudE versus LIS1. GFP-tagged full-length NudE and its deletion constructs were expressed in COS7 cells, treated with nocodazole, and stained with anti-GFP, anti-LIS1, and DAPI. The C-terminal (N189) but not N-terminal (C188) NudE fragment associated with kinetochores. (c) Microtubule organization in LLC-PK1 cells overexpressing NudE fragments revealed severe defects in spindle pole organization after C188 overexpression. No effect was seen in N189-overexpressing cells in comparison with controls. Insets show GFP markers indicating transfection. (d) An LLC-PK1 cell overexpressing a C-terminal fragment of NudE (N189; inset) responsible for kinetochore targeting became arrested in metaphase, as revealed by phase-contrast time-lapse analysis. The chromosomes became pyknotic by 120 min, which is indicative of cell death. (e) Cells overexpressing a C-terminal NudE fragment (N189) showed clear defects in mitotic progression, including mitotic arrest and subsequent cell death (44%), as well as delayed anaphase onset (44%; $n = 16$). (f) Quantitation of the mitotic index for each deletion fragment showed a 15-fold decrease in mitotic cells after the overexpression of NudE-N189 in comparison with controls. No substantial effect was seen with the overexpression of full-length NudE or NudE-C188. Error bars represent the SEM. Bars (b and c), 5 µM; (d) 10 µM.

more pronounced effect on mitotic progression. 44% of cells arrested in metaphase and subsequently underwent cell death, as indicated by nuclear condensation and cell shrinkage (Fig. 4 d), whereas an additional 44% of cells exhibited delayed anaphase onset ($n = 16$; Fig. 4 e). Analysis of the mitotic index in fixed cells expressing the C-terminal NudE fragment revealed a striking decrease in mitotic index. The latter observation is similar to results of ZW10 inhibition (Starr et al., 1998; Chan et al., 2000; Varma et al., 2006) and has been attributed to premature anaphase onset. Our live cell imaging data have revealed a dramatic delay in anaphase onset, and the basis for the reduced mitotic

index in our system is uncertain. No effect on mitotic progression was seen in cells transfected with GFP alone ($n = 6$; Fig. 4 e). In addition, we found the C-terminal fragment of NudE to localize to mitotic kinetochores, which is in contrast to the N-terminal fragment (Fig. 4 b). These results suggest that the C-terminal fragment is necessary for NudE localization to the kinetochore and could compete with full-length NudE or NudEL at this site. We note that the C-terminal fragment also contains a binding site for the early kinetochore protein CENP-F (centromere protein F), which may play a role in NudE and NudEL recruitment to mitotic kinetochores (Soukoulis et al., 2005).

Figure 5. Anti-NudE/NudEL antibody micro-injection causes metaphase arrest. Antibody microinjection was used to inhibit NudE and NudEL function acutely. (a) Time-lapse phase-contrast images of a control LLC-PK1 cell injected with preimmune serum at nuclear envelope breakdown shows normal progression through mitosis. (b) An LLC-PK1 cell injected with anti-NudE/NudEL antibody displays a clear metaphase arrest. By 120 min, DNA decondensation could be observed. (c) Summary of the effects of microinjection. Horizontal bars represent individual cells followed from the time of nuclear envelope breakdown to metaphase (gray) and the duration of metaphase (black). Cells that continued through anaphase are marked with an asterisk. (d) The microinjected NudE/NudEL antibody was imaged using a fluorescent secondary antibody after cell extraction and fixation. The injected antibody is observed at kinetochores, as indicated by double staining with CREST autoimmune serum. Bars (b), 10 μM; (d) 5 μM.
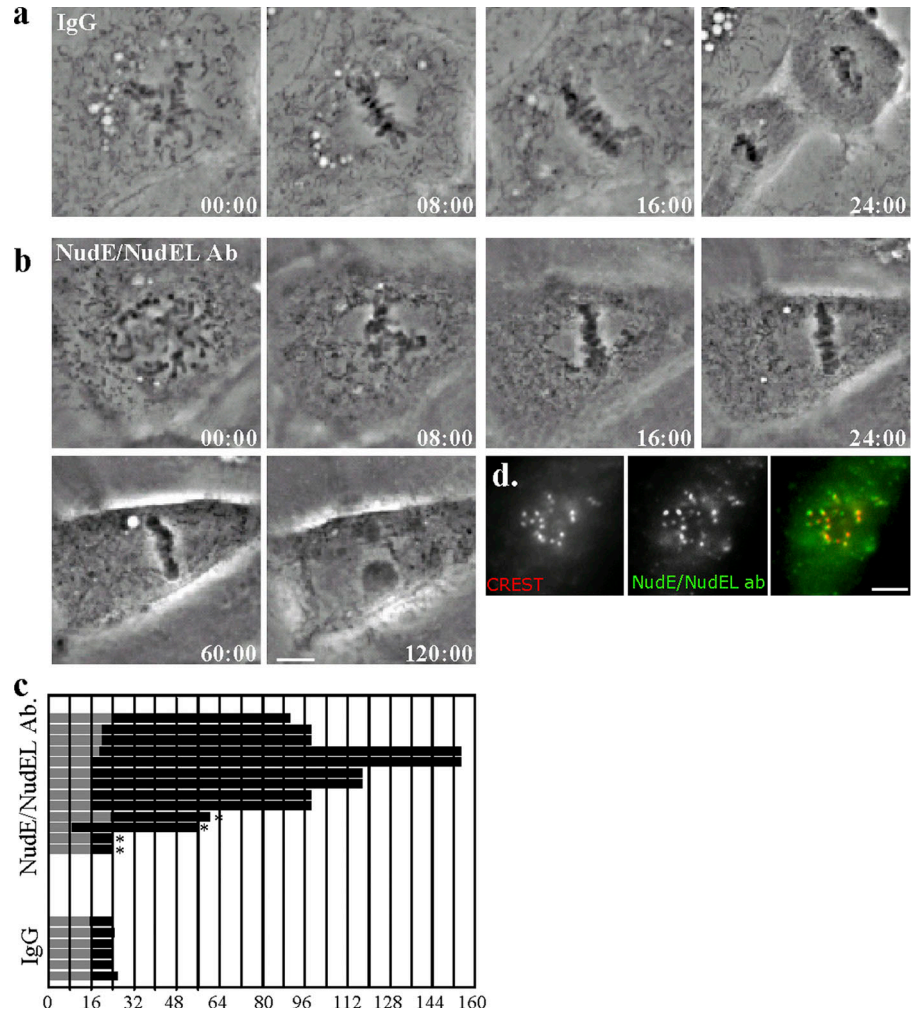
Despite the different patterns of inhibition we observe with the NudE fragments, they are both consistent with the inhibition of cytoplasmic dynein, which is known to participate in spindle organization (Echeverri et al., 1996) as well as the metaphase/anaphase transition. As spindle disorganization is itself likely to affect this transition indirectly, we sought a means for acute NudE and NudEL inhibition to test the specific function of these proteins at kinetochores. In view of the ability of our anti-NudE/NudEL antibody to block the interaction of these proteins with cytoplasmic dynein, we injected it into LLC-PK1 cells during prophase and followed the cells by time-lapse phase-contrast microscopy. 84% of injected cells exhibited a defect in mitotic progression (n = 13; Fig. 5 b), whereas no effect was visible in control cells injected with preimmune serum (n = 6; Fig. 5 a). Metaphase arrest was the most prominent phenotype, occurring in 69% of injected cells. We also examined additional cells that were fixed 60 min after injection and subsequently analyzed for kinetochore composition and orientation (see the next section). Of 80 such cells, 80% exhibited a metaphase-like chromosome configuration. Unlike the effects of LIS1 antibody injection (Faulkner et al., 2000), only minor defects in chromosome congression and the stability of chromosome alignment were evident (15.3%). The majority of arrested cells ultimately showed evidence of cell death; however, a small subset of the cells progressed into anaphase (15.3%; Fig. 5 c).

To identify the site at which the antibody acted, injected cells were preextracted, fixed, and stained with secondary antibody. The injected anti-NudE/NudEL antibody exhibited a clear localization to kinetochores, indicating that endogenous NudE and NudEL were still present at these sites and that inhibition of their interaction with dynein occurred locally (Fig. 5 d).

Effects of NudE/NudEL inhibition on chromosome behavior and kinetochore composition

Although chromosome congression appeared normal by phase-contrast microscopy, more detailed immunofluorescence analysis at 60 min after injection found 61% of cells with evidence of at least one improperly oriented kinetochore pair relative to the spindle axis (n = 23; Fig. 6, a and b). Of the cells containing misoriented kinetochores, 29% contained three or more misoriented pairs. Control cells treated with the proteasome inhibitor MG132 to prevent anaphase onset and subsequently injected with preimmune serum exhibited the proper orientation of almost all kinetochore pairs, although individual misoriented pairs could be detected in a small subset of injected cells (20%; n = 15; Fig. 6, a and b).
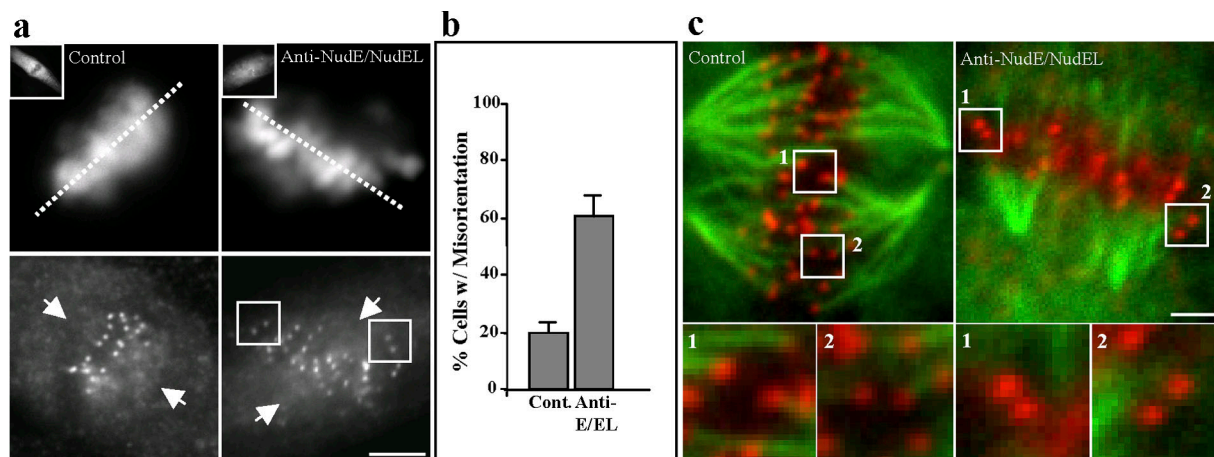
Figure 6. **Effects of anti-NudE/NudEL antibody microinjection on kinetochore orientation and kinetochore microtubule attachment.** (a) Mitotic LLC-PK1 cells were injected with anti-NudE/NudEL antibody at nuclear envelope breakdown and allowed to progress to metaphase. Cells were fixed 1 h after injection and processed for immunofluorescence microscopy. Kinetochore pairs (boxed) showed evidence of misorientation relative to the metaphase plate (dotted lines; positions of the spindle poles are indicated by arrows). Insets show staining for the injected anti-NudE/NudEL antibody as a marker for injection. (b) Fraction of cells showing one or more misoriented kinetochore pairs. Error bars represent the SEM. (c) The stability of microtubule attachment at the kinetochore was examined after a 10-min exposure of anti-NudE/NudEL–injected cells to decreased temperatures (0°C). Although microtubule bundles could still be observed, attachment to individual kinetochores was clearly eliminated in some cases, as shown in boxed areas; these are numbered and shown magnified in the insets. Images of control cells in panels a and c were treated with MG132 to prevent anaphase onset. Bars (a), 5 μM; (c) 3 μM.

In addition, the average distance between sister chromatids in NudE/NudEL antibody–injected cells (1.07 μm; $n = 33$) was substantially shorter than that seen in control cells at metaphase (1.22 μm; $n = 46$). After calculating the distance of unstretched centromeres in nocodazole-treated LLC-PK1 cells (0.58 μm; $n = 47$), the degree of tension in anti-NudE/NudEL antibody–injected cells was found to be 77% of that of controls ([1.07 − 0.58]/[1.22 − 0.58] = 0.77), a decrease similar to that previously seen with dynein inhibition (Howell et al., 2001).

To determine whether the loss of tension was the result of unstable microtubule attachment at kinetochores, antibody-injected cells were subjected to cold treatment to depolymerize nonkinetochore microtubules. The number of kinetochore microtubule bundles appeared substantially decreased, although some bundles were still detected (Fig. 6 c). Examination of individual kinetochores found that many of the misoriented kinetochore pairs lacked microtubule attachments, although examples of unattached but seemingly well-oriented kinetochore pairs were also seen (Fig. 6 c). Whether the loss of kinetochore microtubules reflects a failure in initial attachment or in the stability of attachment is uncertain.

The appearance of NudE and NudEL at kinetochores before dynein, dynactin, LIS1, and ZW10 suggested that NudE and NudEL might function to organize these proteins at mitotic kinetochores. To test the effect of NudE/NudEL inhibition on dynein distribution, we examined antibody-injected cells by immunofluorescence microscopy. Surprisingly, the injected cells showed a complete loss of dynein, dynactin, and LIS1 from all kinetochores, including those on chromosomes that had not yet congressed to the metaphase plate and would normally exhibit strong staining (Fig. 7 a). Quantitative analysis of kinetochore staining showed a 73%, 61%, and 72% reduction for dynein, dynactin, and LIS1, respectively, relative to preimmune-injected

controls (Fig. S3, available at http://www.jcb.org/cgi/content/full/jcb.200610112/DC1). Additionally, antibody injection had no effect on ZW10 or Hec1 kinetochore localization (Figs. 7 a and S3). We also examined kinetochore composition in cells expressing the C-terminal dominant-negative NudE fragment (GFP-NudE-N189). In contrast to the antibody-injected cells, the fragment had no apparent effect on dynactin, LIS1, or ZW10 localization to kinetochores (Fig. S4).

Loss of kinetochore dynein prevents inactivation of the mitotic checkpoint

To determine the status of the mitotic checkpoint in cells in which NudE/NudEL-dependent dynein recruitment has been inhibited, we stained cells injected with the anti-NudE/NudEL antibody for the checkpoint protein BubR1. Strong colocalization of BubR1 and CREST at mitotic kinetochores was detected in all cells examined at both properly oriented and misoriented kinetochores (Fig. 7 a). This result indicates that the NudE/NudEL-dependent loss of dynein prevents checkpoint protein removal even on kinetochores that have congressed to the metaphase plate.

Although BubR1 levels have been shown to decrease on fully aligned metaphase chromosomes, Mad2 provides a more definitive indication of the mitotic checkpoint status, as it shows a greater depletion on aligned kinetochores (Hoffman et al., 2001) and is removed from kinetochores in a dynein-dependent manner (Howell et al., 2001). Because of the difficulty in imaging Mad2 by immunofluorescence in anti-NudE/NudEL–injected cells, we performed sequential injections with anti-NudE/NudEL and anti-Mad2 antibodies and imaged cells using time-lapse phase-contrast microscopy. Cells were observed to enter anaphase ∼10 min after the second injection, indicating that the Mad2-dependent checkpoint was responsible for anti-NudE/NudEL–induced metaphase arrest ($n = 5$). In addition, cells
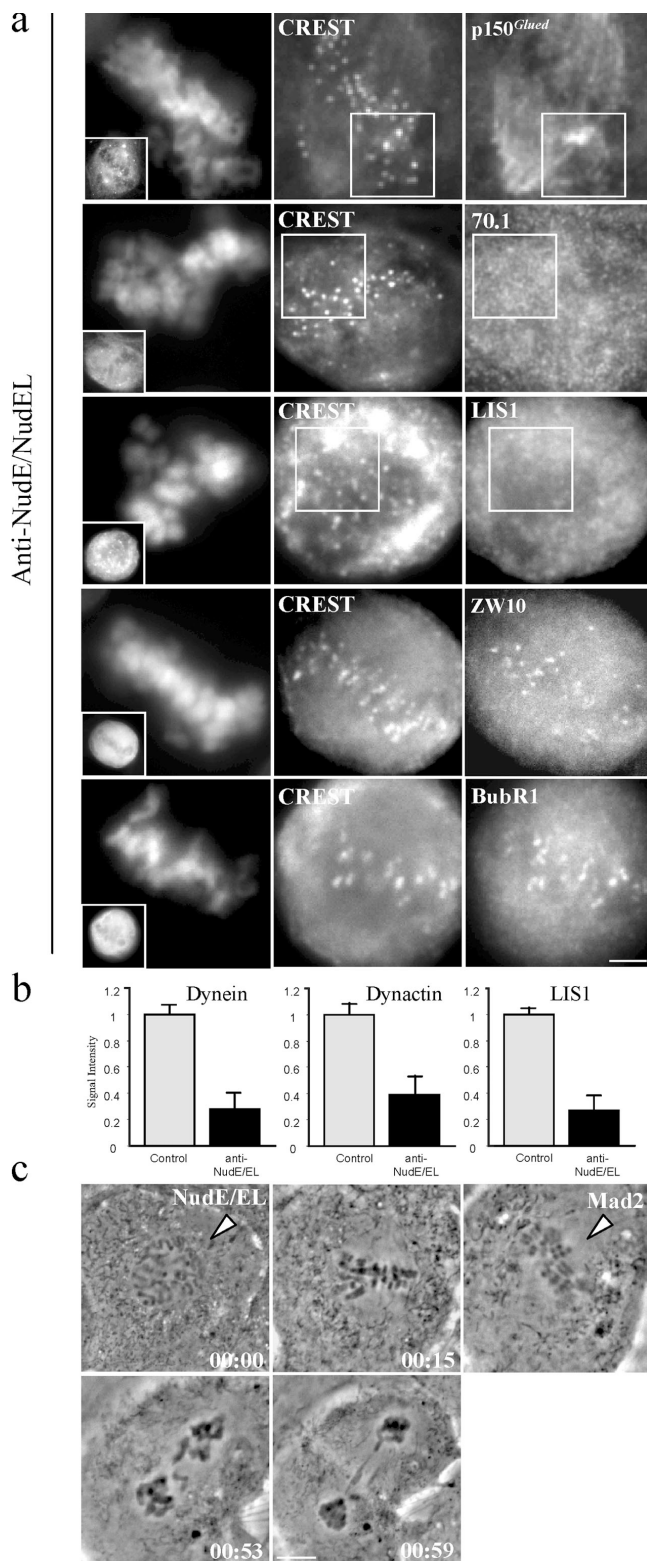
a

	CREST	p150^Glued
CREST	70.1
CREST	LIS1
CREST	ZW10
CREST	BubR1

Anti-NudE/NudEL

b

Dynein · Dynactin · LIS1

c

NudE/EL · Mad2
00:00 · 00:15
00:53 · 00:59

exhibited lagging chromosomes during this precocious anaphase onset, which is consistent with our findings that kinetochore microtubule attachment was incomplete or unstable (Fig. 7 c).

NudE interacts with the cytoplasmic dynein intermediate chain and light chain

Although NudEL has been reported to interact with the cytoplasmic dynein motor domain (Sasaki et al., 2000), this type of interaction seems inconsistent with a role for NudE and NudEL in anchoring the motor protein to kinetochores. To define the mechanism by which dynein, NudE, and NudEL interact, we tested the ability of recombinant NudE to bind to a well-behaved recombinant rat cytoplasmic dynein motor domain (Hook et al., 2005) as well as the cytoplasmic dynein complex purified from brain tissue (Paschal et al., 1987). Although the purified dynein complex exhibited a clear interaction with NudE (Fig. 8 a), as was found for dynein in brain cytosolic extract (Fig. 1 a), no interaction with the recombinant motor domain could be detected (Fig. 8 a). These data suggested that the interaction with the dynein complex might be through its stem, or tail, domain. To test this possibility, we performed GST-NudE pulldowns from COS7 cells transfected with cDNAs encoding individual dynein subunits. We observed a clear, strong interaction with both the dynein intermediate chain IC2C and the light chain LC8 (Fig. 8 b). No interaction was seen with the cytoplasmic dynein light intermediate chains LIC1 and LIC2 or a 1,137-aa fragment of the cytoplasmic dynein heavy chain corresponding to the entire base region of the molecule (Fig. 8 b).

Discussion

We have found that despite the dramatic differences in brain developmental phenotypes reported for NudE and NudEL (Feng and Walsh, 2004; Sasaki et al., 2005), they each localize prominently to mitotic kinetochores. Unlike LIS1, they appear at this site earlier than dynein, dynactin, LIS1, and ZW10. Injection of an antibody that blocks the interaction of NudE and NudEL with cytoplasmic dynein displaced the motor protein along with dynactin and LIS1 from kinetochores. Antibody injection resulted in checkpoint-dependent metaphase arrest, with novel defects in kinetochore orientation. Surprisingly, NudE interacted not with the dynein motor domain but with both the intermediate chain IC2C and the light chain LC8. Collectively, these results identify a novel role for NudE and NudEL in kinetochore organization and reveal an alternative mechanism for dynein targeting from that involving ZW10.

Figure 7. **Analysis of the composition and functional state of kinetochores in anti-NudE/NudEL antibody–injected cells.** (a) LLC-PK1 cells were injected with anti-NudE/NudEL antibody at nuclear envelope breakdown, fixed after 60 min, and examined by immunofluorescence microscopy. NudE/NudEL antibody injection displaced both dynactin (p150^Glued), dynein (70.1), and LIS1 from mitotic kinetochores as indicated by the loss of colocalization with CREST. Uncongressed chromosomes still in a pro-metaphase-like state were used in this analysis, as indicated by boxed regions. No effect on ZW10 or BubR1 localization to the kinetochore was seen in antibody-injected HeLa cells. Insets show staining for injected anti-NudE/NudEL antibody as a marker for injection. (b) Quantitative analysis of kinetochore staining signal intensity in anti-NudE/NudEL antibody–injected cells showed a 73%, 61%, and 72% reduction for dynein, dynactin, and LIS1, respectively, relative to preimmune-injected controls. Error bars represent the SEM. (c) The Mad2-dependent mitotic checkpoint is still active in anti-NudE/NudEL antibody–injected LLC-PK1 cells. Sequential injections were first performed with an anti-NudE/NudEL antibody and then with an anti-Mad2 antibody. Cells underwent precocious anaphase onset ~10 min after the second injection, as indicated by lagging chromosomes (n = 5). Arrows indicate the injection of each antibody as labeled in the figure. Bars (a), 5 μM; (c) 10 μM.
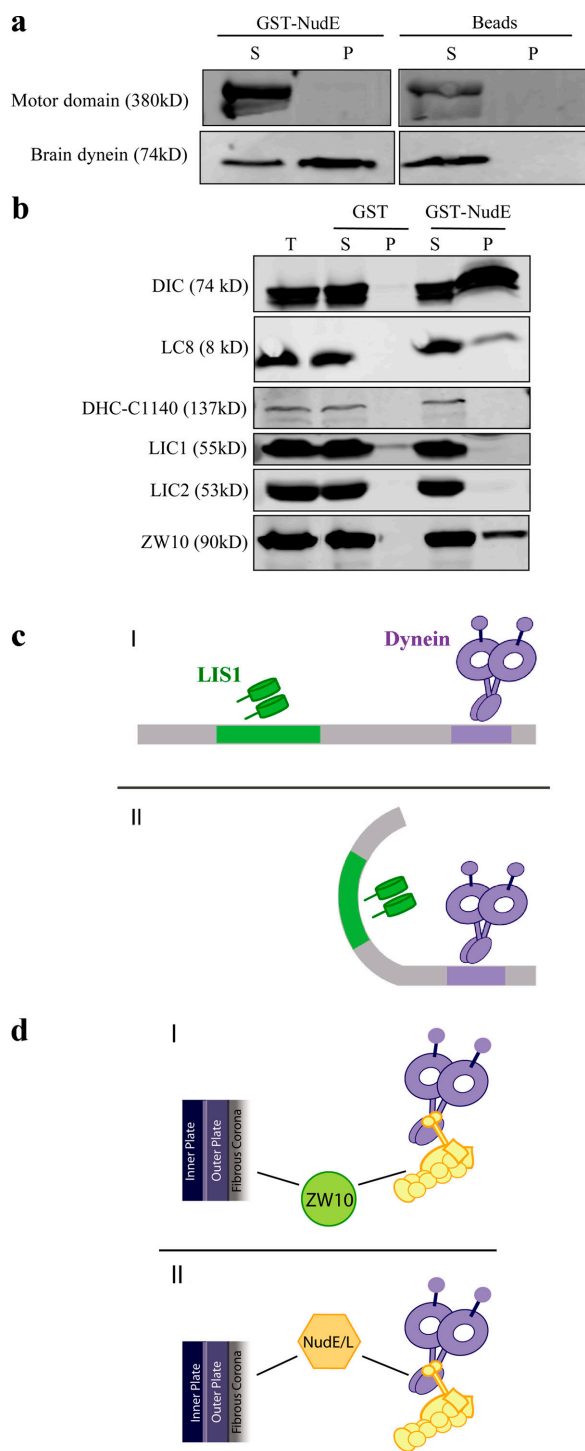
Figure 8. NudE interactions. (a) GST-NudE pulldowns of recombinant cytoplasmic dynein motor domain versus purified brain cytoplasmic dynein holoenzyme. Only the latter bound to the bacterially expressed GST-NudE. (b) GST-NudE pulldowns from COS7 lysate overexpressing dynein subunits, a dynein heavy chain stem fragment (DHC-C1140; Gee et al., 1997), and ZW10. An interaction was seen with the cytoplasmic dynein intermediate chain IC2C, light chain LC8, and ZW10. (c) Dynein regulation during mitosis may be dependent on the ability of NudE to interact with both LIS1 and dynein. (I) Schematic representation of the NudE–LIS1 interaction as well as our newly identified interaction between NudE and the base of the dynein molecule. (II) Overexpression of a NudE fragment responsible for kinetochore targeting (N189) and anti-NudE/NudEL antibody injection both result in metaphase arrest, although dynein localization to the kinetochore is only lost in the latter case. This indicates that full-length NudE must

Subcellular localization of NudE and NudEL

The physiological relationship between NudE and NudEL has been uncertain. Despite their similarity in primary structural organization, the developmental phenotypes produced by gene knockout are very different (Feng and Walsh, 2004; Sasaki et al., 2005). The extent to which this outcome reflects differences in the temporal and spatial expression pattern versus functional specificity is unknown. We find that heterologously expressed GFP-NudE and -NudEL each target to mitotic kinetochores. These results support our immunocytochemical evidence of NudE/NudEL kinetochore localization using an antibody that reacts with both proteins, and, combined, these data strongly suggest that the cellular functions of NudE and NudEL are, in fact, closely related.

Evidence that the structures we observe within the mitotic spindle are kinetochores comes from double labeling with a variety of markers as well as phenotypic analysis. We find that both NudE and NudEL associated with the outer kinetochore coincident with the location of cytoplasmic dynein, dynactin, and LIS1 and external to the CREST autoantigens, which are associated with the inner kinetochore. Using our anti-NudE/NudEL antibody, we find that the proteins appear at the kinetochore before dynein, dynactin, and LIS1. Using GFP-tagged forms of each protein, surprisingly, we find that NudE and NudEL kinetochore localization also precedes that of ZW10, a known dynein-interacting protein that has been found to be necessary for the association of dynein and dynactin with the kinetochore. The early appearance of NudE and NudEL at this site provides the first indication that these two proteins may act upstream of other dynein accessory proteins in this pathway and may play a role in dynein recruitment to the kinetochore. NudE and NudEL also depart the kinetochore after dynein, dynactin, and LIS1, further supporting an independent mode of attachment for NudE and NudEL to the kinetochore, which is resistant to the proposed dynein-dependent removal at the time of microtubule attachment. We saw no apparent localization of N-terminal NudE fragments to the kinetochore, indicating that the protein is not recruited to this site via LIS1, which interacts with this part of the NudE molecule. In contrast, we observed clear kinetochore binding by a C-terminal NudE fragment. This part of NudE contains a binding site for cytoplasmic dynein and was also found to be sufficient for centrosome localization (Guo et al., 2006), suggesting that common elements of the molecule may be involved in targeting to multiple functional sites. We note that the C-terminal fragment of NudE also contains a binding site for CENP-F, a known early kinetochore protein that could play a role in NudE recruitment to mitotic kinetochores.

In addition to temporal differences in kinetochore localization, we observed differences in the distribution of NudE and NudEL from dynein and its other regulatory factors at the

interact with both LIS1 and dynein for proper dynein regulation during mitosis. (d) Proposed kinetochore function of NudE/NudEL during mitosis. (I) Conventional model for dynein anchorage to the kinetochore through dynactin and ZW10. (II) Organization of kinetochore proteins based on this study identifying a new, complementary role for NudE/NudEL in this process. T, total; S, supernatant; P, pellet.

cell cortex. NudE/NudEL immunoreactivity appeared at sites of cell–cell contact in partially polarized epithelial cells, although we were unable to discern a specific association with adherens junctions as has been previously reported for cytoplasmic dynein (Ligon et al., 2001). In further contrast to dynein, dynactin, and LIS1, we did not detect NudE/NudEL at the mitotic cell cortex, although dynein and LIS1 association with this site has been implicated in mitotic spindle orientation (Busson et al., 1998; Faulkner et al., 2000). The absence of NudE and NudEL from this region of the dividing cell implies that these proteins are not required for dynein or LIS1 recruitment to the mitotic cortex and that, in contrast to LIS1 (Faulkner et al., 2000), spindle orientation is unlikely to be under the control of either NudE or NudEL.

Mitotic functions of NudE and NudEL

We used several approaches to examine the role of NudE and NudEL in mitotic function. Because NudE and NudEL RNAi results in a severe mitotic cell death phenotype, we focused on the use of dominant-negative and function-blocking antibody probes for phenotypic analysis. As previously described, the expression of N-terminal NudE fragments had pronounced effects on mitotic spindle morphology, leading to defects in mitotic progression (Feng et al., 2000; Feng and Walsh, 2004). Overexpression of the C-terminal half of NudE was reported to have no apparent effect on spindle morphology or mitotic index (Feng and Walsh, 2004). Nonetheless, we observed a pronounced metaphase arrest after overexpression and an almost 15-fold decrease in mitotic index as determined by immunocytochemical analysis. Spindle disruption was not observed, suggesting that the effects on kinetochore function are direct.

As an additional means of minimizing indirect phenotypic effects and to inhibit NudE and NudEL acutely, we microinjected our anti-NudE/NudEL antibody into dividing cells. NudE and NudEL are each known to interact with dynein and LIS1, which we confirmed in pulldown assays. We observed no interaction with dynactin or NudC, the latter results suggesting potential complementary roles for NudE/NudEL versus NudC in LIS1-dynein behavior. Our polyclonal anti-NudE/NudEL antibody immunoprecipitated LIS1 and ZW10 but not dynein, suggesting that the antibody specifically interferes with the dynein interaction site within NudE and NudEL.

When injected into cells, the antibody interfered with mitotic progression, producing a severe metaphase arrest. This effect was very similar to that observed from expression of the C-terminal NudE fragment. As in that case, and in contrast to the N-terminal NudE fragment, the antibody had no apparent effect on spindle organization. In addition, the injected antibody remained at the kinetochore, indicating that NudE and NudEL were not displaced. However, dynein, dynactin, and LIS1 were missing from these sites. Chromosome congression in the injected cells occurred normally both in terms of the time required for this process to complete and in the uniform alignment of chromosomes at the metaphase plate. These results provide further support for the contention that dynein is not required for congression, a role that has been ascribed to another microtubule motor protein, CENP-E (Kapoor et al., 2006). The majority

of the arrested cells remained at metaphase for prolonged periods of time, which is consistent with the effects of acute dynein and dynactin inhibition by the microinjection of antidynein antibody or recombinant dynamitin (Howell et al., 2001). We did not observe the unstable alignment phenotype we previously reported for anti-LIS1 antibody–injected cells in which chromosomes departed and rejoined the metaphase plate after alignment (Faulkner et al., 2000). Several of those cells also entered anaphase before complete alignment, suggesting a partial mitotic checkpoint defect (Faulkner et al., 2000). In the present study, we judged the mitotic checkpoint to remain active in anti-NudE/NudEL–injected cells by use of a subsequent anti-Mad2 antibody injection that induced precocious anaphase onset.

As judged by kinetochore spacing, tension between paired kinetochores was decreased, although not eliminated, in the anti-NudE/NudEL antibody–injected cells. More striking were errors in kinetochore orientation relative to the plane of the metaphase plate, which have not been reported for LIS1-, dynein-, or dynactin-inhibited cells and suggest an additional role for NudE and NudEL in proper microtubule attachment. To further test this possibility, we exposed antibody-injected cells to decreased temperatures and found that the number of kinetochore microtubule bundles were deceased, which is consistent with a microtubule attachment defect. We note that although all kinetochores in the injected cells lacked dynein and dynactin, only a few were clearly misoriented. This observation suggests that sister chromatid orientation may remain dynamic in the injected cells. BubR1 was also retained on kinetochores in the antibody-injected cells, which is a result consistent with improper microtubule attachment. Together, these data are the first to implicate the cytoplasmic dynein pathway in stable microtubule attachment to kinetochores.

The active mitotic checkpoint in anti-NudE/NudEL antibody–injected cells could be the result of the loss of kinetochore dynein, defective microtubule attachment, or both. This persistent activation seems more likely to be a direct reflection of the inability of dynein to remove checkpoint proteins from kinetochores, an activity described in previous studies (Howell et al., 2001; Wojcik et al., 2001).

Molecular interactions

NudEL pulled out two fragments of the dynein motor domain in a yeast two-hybrid library screen (Sasaki et al., 2000). However, the loss of cytoplasmic dynein from kinetochores in anti-NudE/NudEL antibody–injected cells is difficult to reconcile with a motor domain interaction, which would not be expected to affect dynein recruitment to the kinetochore. Instead, we did detect strong interactions with a dynein intermediate and light chain, which reside at the base of the dynein molecule and have been implicated in dynein anchorage and cargo binding. Although our data cannot rule out an interaction between NudE or NudEL and the dynein motor domain, we conclude that anti-NudE/NudEL antibody injection interferes not with dynein motor function but rather with dynein targeting (Fig. 8 c). We also note that overexpression of the C-terminal NudE fragment produces a similar phenotype to that generated by anti-NudE/NudEL antibody injection despite the retention of dynein, dynactin, and

LIS1 at kinetochores in these cells. Because the fragment itself associates with kinetochores, we suspect that it may displace endogenous full-length NudE, and the resulting phenotype may indicate that both the LIS1 and dynein-binding sites must be linked within the same NudE molecule for proper dynein regulation (Fig. 8 c).

This result is particularly surprising in view of long-standing evidence that ZW10, through dynactin, is necessary for dynein binding to the kinetochore (Starr et al., 1998; Kops et al., 2005). ZW10 was not displaced from kinetochores by NudE/NudEL antibody injection, further indicating that these proteins are independently required for dynein recruitment to the kinetochore. Conceivably, ZW10 and NudE or NudEL cooperate in dynein recruitment, and each is necessary for dynein to remain associated with the kinetochore. In this view, however, dynactin should be unaffected by anti-NudE/NudEL injection, as this complex interacts with ZW10 but not with NudE, as shown here (Fig. 1 a). Surprisingly, we find dynactin to be displaced by antibody injection despite the persistence of ZW10 at the kinetochore. This result could reflect steric hindrance of the injected NudE/NudEL antibody on the interaction between dynactin and ZW10. Alternatively, it may also imply that dynactin can exist in a state in which it is primarily tethered to the kinetochore through its interaction with dynein (Fig. 8 d). The latter possibility suggests that NudE/NudEL and ZW10 play complementary and potentially independent roles in dynein recruitment (Fig. 8 d). How these interactions are coordinated and how they relate to the maturation of the microtubule–kinetochore link remain important issues for further investigation.

Materials and methods

Cell culture and immunocytochemistry
COS7, MDCK, and HeLa cells were grown in DME supplemented with 10% FBS, LLC-PK1 cells were grown in DME supplemented with 3% FBS, and NIH-3T3 fibroblasts were grown in DME supplemented with 10% bovine calf serum. Transient transfections were performed using Effectene (QIAGEN). Full-length NudE and NudEL as well as the NudE-C188 and NudE-N189 deletion constructs were each cloned from a mouse cDNA library using the Marathon cDNA Amplification kit (CLONTECH Laboratories, Inc.) into pEGFP-C1 (CLONTECH Laboratories, Inc.). The IC2C-myc, HC-C1140-myc, LIC1-HA, LIC2-FLAG, and LC8-VSVG constructs were described previously (Vaughan and Vallee, 1995; Tynan et al., 2000a,b; Tai et al., 2002). We generated a polyclonal rabbit antibody against bacterially expressed full-length mNudE. Additional antibodies used included polyclonal anti-Arp1 (provided by D. Meyer, University of California, Los Angeles, Los Angeles, CA), monoclonal anti-p150^{Glued} (BD Biosciences), polyclonal anti-LIS1 (Santa Cruz Biotechnology, Inc.), monoclonal anti-LIS1 (provided by O. Reiner, Weizmann Institute, Rehovot, Israel), monoclonal anti-BUBR1 (BD Biosciences), chicken anti-GFP (Chemicon), monoclonal HEC1 (Abcam), polyclonal anti–ZW10-Cter (Varma et al., 2006), rat monoclonal tyrosinated anti–α-tubulin (YL1/2; Kilmartin et al., 1982; Gomes et al., 2004), monoclonal anti-dynein intermediate chain (clone 70.1; Sigma-Aldrich), and human CREST autoimmune serum (Antibodies, Inc.). To generate stable cell lines, full-length NudE and NudEL were cloned into the localization and affinity purification vector pIC113. Individual colonies were screened for endogenous levels of expression and kept under stable selection.

Biochemical and molecular analysis
Full-length NudE was cloned into pGEX6p-1 (GE Healthcare) and purified from bacteria by glutathione-Sepharose affinity chromatography. Bovine brain lysate and cytoplasmic dynein were prepared as previously described in phosphate-glutamate buffer (Paschal et al., 1987). Individual dynein subunits or fragments were expressed in COS7 cells. Pulldowns were performed by adsorbing GST-NudE to glutathione-Sepharose and rocking gently for 1–2 h in the presence of bovine brain extract, 2.5 μg of purified cytoplasmic dynein (∼6 nM), 10 μg of purified motor domain (∼75 nM), or transfected cell lysate. Immunoprecipitations from bovine brain extract were performed by overnight incubation using protein A–Sepharose. NudE- and NudEL-interacting proteins were identified by immunoblotting. Total RNA was isolated from cell lysates using the Absolutely RNA RT-PCR Miniprep kit (Stratagene), processed using RETROscript (Ambion), and analyzed by agarose gel electrophoresis.

Immunofluorescence microscopy
Cells were preextracted using 0.1% Triton X-100 in PHEM buffer (120 mM Pipes, 50 mM Hepes, 20 mM EGTA, and 4 mM magnesium acetate) for 30 s, fixed in 3% PFA in PHEM buffer for 20 min, and fixed in methanol at −20°C for 6 min (Busson et al., 1998). Coverslips were blocked for 30 min with 0.5% BSA, incubated for 1 h in primary antibody, washed, and incubated for 1 h using Cy2-, Cy3-, and Cy5-conjugated secondary antibodies (Jackson ImmunoResearch Laboratories). To stain chromosomes, cells were subsequently exposed to DAPI for 10 min and mounted using ProLong Gold antifade reagent (Invitrogen). Cells were then visualized on an inverted microscope (described below) or by confocal imaging (510 META; Carl Zeiss MicroImaging, Inc.). Analysis of kinetochore orientation and microtubule attachment was performed on 3D stacks that were acquired using a spinning disk confocal microscope (DSU; Olympus) on an inverted microscope (IX80; Olympus).

Microinjection and live cell imaging
For all antibody injection experiments, a purified IgG fraction of our anti-NudE/NudEL polyclonal antibody was concentrated in microinjection buffer (8–15 mg ml^{-1} in 50 mM potassium glutamate containing 0.5 mM MgCl$_2$, pH 7.0). Preimmune IgG serum was used in control injections of cells treated with 10 μM MG132. Cells were visualized at 37°C in a 5% CO$_2$ atmosphere using an inverted microscope equipped with an incubation chamber (DMIRBE; Leica) and injected during prophase. For live cell analysis, images were collected every 4 min after injection for up to 120 min with a CCD camera (ORCA 100; Hamamatsu) piloted by MetaMorph (Universal Imaging Corp.).

Online supplemental material
Fig. S1 includes additional information on the biochemical analysis of our polyclonal anti-NudE/NudEL antibody. Fig. S2 shows the distinct mitotic localization of GFP-NudEL in comparison with LIS1 and ZW10. Fig. S3 contains images of kinetochore composition in preimmune-injected control cells. Fig. S4 demonstrates the effects of NudE-N189 overexpression on kinetochore composition. Online supplemental material is available at http://www.jcb.org/cgi/content/full/jcb.200610112/DC1.

References

Busson, S., D. Dujardin, A. Moreau, J. Dompierre, and J.R. De Mey. 1998. Dynein and dynactin are localized to astral microtubules and at cortical sites in mitotic epithelial cells. *Curr. Biol.* 8:541–544.

Chan, G.K., S.A. Jablonski, D.A. Starr, M.L. Goldberg, and T.J. Yen. 2000. Human Zw10 and ROD are mitotic checkpoint proteins that bind to kinetochores. *Nat. Cell Biol.* 2:944–947.

Dujardin, D.L., L.E. Barnhart, S.A. Stehman, E.R. Gomes, G.G. Gundersen, and R.B. Vallee. 2003. A role for cytoplasmic dynein and LIS1 in directed cell movement. *J. Cell Biol.* 163:1205–1211.

Echeverri, C.J., B.M. Paschal, K.T. Vaughan, and R.B. Vallee. 1996. Molecular characterization of the 50kD subunit of dynactin reveals function for the complex in chromosome alignment and spindle organization during mitosis. *J. Cell Biol.* 132:617–633.

Efimov, V.P., and N.R. Morris. 2000. The LIS1-related NUDF protein of *Aspergillus nidulans* interacts with the coiled-coil domain of the NUDE/RO11 protein. *J. Cell Biol.* 150:681–688.

Efimov, V.P., J. Zhang, and X. Xiang. 2006. CLIP-170 homologue and NUDE play overlapping roles in NUDF localization in *Aspergillus nidulans*. *Mol. Biol. Cell*. 17:2021–2034.

Faulkner, N.E., D.L. Dujardin, C.Y. Tai, K.T. Vaughan, C.B. O'Connell, Y. Wang, and R.B. Vallee. 2000. A role for the lissencephaly gene LIS1 in mitosis and cytoplasmic dynein function. *Nat. Cell Biol.* 2:784–791.

Feng, Y., and C.A. Walsh. 2004. Mitotic spindle regulation by nde1 controls cerebral cortical size. *Neuron.* 44:279–293.

Feng, Y., E.C. Olson, P.T. Stukenberg, L.A. Flanagan, M.W. Kirschner, and C.A. Walsh. 2000. LIS1 regulates CNS lamination by interacting with mNudE, a central component of the centrosome. *Neuron.* 28:665–679.

Gee, M.A., J.E. Heuser, and R.B. Vallee. 1997. An extended microtubule-binding structure within the dynein motor domain. *Nature.* 390:636–639.

Gomes, E.R., S. Jani, and G.G. Gundersen. 2005. Nuclear movement regulated by Cdc42, MRCK, myosin, and actin flow establishes MTOC polarization in migrating cells. *Cell.* 121:451–463.

Guo, J., Z. Yang, W. Song, Q. Chen, F. Wang, Q. Zhang, and X. Zhu. 2006. Nudel contributes to microtubule anchoring at the mother centriole and is involved in both dynein-dependent and -independent centrosomal protein assembly. *Mol. Biol. Cell.* 17:680–689.

Harada, A., Y. Takei, Y. Kanai, Y. Tanaka, S. Nonaka, and N. Hirokawa. 1998. Golgi vesiculation and lysosome dispersion in cells lacking cytoplasmic dynein. *J. Cell Biol.* 141:51–59.

Hirohashi, Y., Q. Wang, Q. Liu, B. Li, X. Du, H. Zhang, K. Furuuchi, K. Masuda, N. Sato, and M.I. Greene. 2006. Centrosomal proteins Nde1 and Su48 form a complex regulated by phosphorylation. *Oncogene.* 25:6048–6055.

Hirotsune, S., M.W. Fleck, M.J. Gambello, G.J. Bix, A. Chen, G.D. Clark, D.H. Ledbetter, C.J. McBain, and A. Wynshaw-Boris. 1998. Graded reduction of *Pafah1b1* (*Lis1*) activity results in neuronal migration defects and early embryonic lethality. *Nat. Genet.* 19:333–339.

Hoffman, D.B., C.G. Pearson, T.J. Yen, B.J. Howell, and E.D. Salmon. 2001. Microtubule-dependent changes in assembly of microtubule motor proteins and mitotic spindle checkpoint proteins at PtK1 kinetochores. *Mol. Biol. Cell.* 12:1995–2009.

Hook, P., A. Mikami, B. Shafer, B.T. Chait, S.S. Rosenfeld, and R.B. Vallee. 2005. Long range allosteric control of cytoplasmic dynein ATPase activity by the stalk and C-terminal domains. *J. Biol. Chem.* 280:33045–33054.

Howell, B.J., B.F. McEwen, J.C. Canman, D.B. Hoffman, E.M. Farrar, C.L. Rieder, and E.D. Salmon. 2001. Cytoplasmic dynein/dynactin drives kinetochore protein transport to the spindle poles and has a role in mitotic spindle checkpoint inactivation. *J. Cell Biol.* 155:1159–1172.

Kapoor, T.M., M.A. Lampson, P. Hergert, L. Cameron, D. Cimini, E.D. Salmon, B.F. McEwen, and A. Khodjakov. 2006. Chromosomes can congress to the metaphase plate before biorientation. *Science.* 311:388–391.

Kilmartin, J., B. Wright, and C. Milstein. 1982. Rat monoclonal antitubulin antibodies derived by using a new nonsecreting rat cell line. *J. Cell Biol.* 93:576–582.

Kops, G.J., Y. Kim, B.A. Weaver, Y. Mao, I. McLeod, J.R. Yates, M. Tagaya, and D.W. Cleveland. 2005. ZW10 links mitotic checkpoint signaling to the structural kinetochore. *J. Cell Biol.* 169:49–60.

Li, J., W.-L. Lee, and J.A. Cooper. 2005. NudEL targets dynein to microtubule ends through LIS1. *Nat. Cell Biol.* 7:686–690.

Liang, Y., W. Yu, Y. Li, Z. Yang, X. Yan, Q. Huang, and X. Zhu. 2004. Nudel functions in membrane traffic mainly through association with Lis1 and cytoplasmic dynein. *J. Cell Biol.* 164:557–566.

Ligon, L.A., S. Karki, M. Tokito, and E.L. Holzbaur. 2001. Dynein binds to beta-catenin and may tether microtubules at adherens junctions. *Nat. Cell Biol.* 3:913–917.

Niethammer, M., D.S. Smith, R. Ayala, J. Peng, J. Ko, M.S. Lee, M. Morabito, and L.H. Tsai. 2000. NUDEL is a novel Cdk5 substrate that associates with LIS1 and cytoplasmic dynein. *Neuron.* 28:697–711.

O'Connell, C.B., and Y. Wang. 2000. Mammalian spindle orientation and position respond to changes in cell shape in a dynein-dependent fashion. *Mol. Biol. Cell.* 11:1765–1774.

Paschal, B.M., and R.B. Vallee. 1987. Retrograde transport by the microtubule associated protein MAP 1C. *Nature.* 330:181–183.

Paschal, B.M., H.S. Shpetner, and R.B. Vallee. 1987. MAP 1C is a microtubule-activated ATPase which translocates microtubules in vitro and has dynein-like properties. *J. Cell Biol.* 105:1273–1282.

Sasaki, S., A. Shionoya, M. Ishida, M.J. Gambello, J. Yingling, A. Wynshaw-Boris, and S. Hirotsune. 2000. A LIS1/NUDEL/cytoplasmic dynein heavy chain complex in the developing and adult nervous system. *Neuron.* 28:681–696.

Sasaki, S., D. Mori, K. Toyo-oka, A. Chen, L. Garrett-Beal, M. Muramatsu, S. Miyagawa, N. Hiraiwa, A. Yoshiki, A. Wynshaw-Boris, and S. Hirotsune. 2005. Complete loss of Ndel1 results in neuronal migration defects and early embryonic lethality Mol. *Mol. Cell. Biol.* 25:7812–7827.

Shu, T., R. Ayala, M.D. Nguyen, Z. Xie, J.G. Gleeson, and L.H. Tsai. 2004. Ndel1 operates in a common pathway with LIS1 and cytoplasmic dynein to regulate cortical neuronal positioning. *Neuron.* 44:263–277.

Smith, D.S., M. Niethammer, R. Ayala, Y. Zhou, M.J. Gambello, A. Wynshaw-Boris, and L.H. Tsai. 2000. Regulation of cytoplasmic dynein behaviour and microtubule organization by mammalian Lis1. *Nat. Cell Biol.* 2:767–775.

Soukoulis, V., S. Reddy, R.D. Pooley, Y. Feng, C.A. Walsh, and D.M. Bader. 2005. Cytoplasmic LEK1 is a regulator of microtubule function through its interaction with the LIS1 pathway. *Proc. Natl. Acad. Sci. USA.* 102:8549–8554.

Starr, D.A., B.C. Williams, T.S. Hays, and M.L. Goldberg. 1998. ZW10 helps recruit dynactin and dynein to the kinetochore. *J. Cell Biol.* 142:763–774.

Starr, D.A., R. Saffery, Z. Li, A.E. Simpson, K.H. Choo, T.J. Yen, and M.L. Goldberg. 2000. HZwint-1, a novel human kinetochore component that interacts with HZW10. *J. Cell Sci.* 113:1939–1950.

Tai, C.Y., D.L. Dujardin, N.E. Faulkner, and R.B. Vallee. 2002. Role of dynein, dynactin, and CLIP-170 interactions in LIS1 kinetochore function. *J. Cell Biol.* 156:959–968.

Tsai, J.-W., Y. Chen, A.R. Kriegstein, and R.B. Vallee. 2005. LIS1 RNA interference blocks neural stem cell division, morphogenesis, and motility at multiple stages. *J. Cell Biol.* 170:935–945.

Tynan, S.H., M.A. Gee, and R.B. Vallee. 2000a. Distinct but overlapping sites within the cytoplasmic dynein heavy chain for dimerization and for intermediate chain and light intermediate chain binding. *J. Biol. Chem.* 275:32769–32774.

Tynan, S.H., A. Purohit, S.J. Doxsey, and R.B. Vallee. 2000b. Light intermediate chain 1 defines a functional subfraction of cytoplasmic dynein which binds to pericentrin. *J. Biol. Chem.* 275:32763–32768.

Varma, D., D.L. Dujardin, S.A. Stehman, and R.B. Vallee. 2006. Role of the kinetochore/cell cycle checkpoint protein ZW10 in interphase cytoplasmic dynein function. *J. Cell Biol.* 172:655–662.

Vaughan, K., and R. Vallee. 1995. Cytoplasmic dynein binds dynactin through a direct interaction between the intermediate chains and p150Glued. *J. Cell Biol.* 131:1507–1516.

Wojcik, E., R. Basto, M. Serr, F. Scaerou, R. Karess, and T. Hays. 2001. Kinetochore dynein: its dynamics and role in the transport of the Rough deal checkpoint protein. *Nat. Cell Biol.* 3:1001–1007.

Xiang, X., A.H. Osmani, S.A. Osmani, M. Xin, and N.R. Morris. 1995. NudF, a nuclear migration gene in *Aspergillus nidulans*, is similar to the human LIS-1 gene required for neuronal migration. *Mol. Biol. Cell.* 6:297–310.

Yan, X., F. Li, Y. Liang, Y. Shen, X. Zhao, Q. Huang, and X. Zhu. 2003. Human Nudel and NudE as regulators of cytoplasmic dynein in poleward protein transport along the mitotic spindle. *Mol. Cell. Biol.* 23:1239–1250.